Supplement of Atmos. Chem. Phys., 24, 4411–4419, 2024
https://doi.org/10.5194/acp-24-4411-2024-supplement

Atmospheric Chemistry and Physics
Open Access

Supplement of

Technical Note: A technique to convert NO_2 to NO_2^- with S(IV) and its application to measuring nitrate photolysis

Aaron Lieberman et al.

Correspondence to: Cort Anastasio (canastasio@ucdavis.edu)

Table of Contents

Section S1. Materials and Solution Preparation

Sodium nitrate (ACS grade), sodium sulfite (ACS grade), 2-propanol (ACS plus grade), potassium phosphate monobasic (ACS grade), sodium hydroxide (ACS grade), and hydrochloric acid (trace metal grade) were purchased from Fisher Scientific. Sodium nitrite (99.9995%) was purchased from Thermos Scientific. Sulfanilamide (99%), N-(1-napthyl)ethylenediamine dihydrochloride (NED) (reagent grade), and hydrogen peroxide (H_2O_2) (30% solution) were purchased from Sigma Aldrich.

All solutions were prepared with water from a Milli-Q (MQ) Advantage A10 system (18.2 MΩ cm) with an upstream carbon cartridge (Barnstead) that kept TOC < 5 ppb. Illumination solutions were prepared with 50 µM sodium nitrate, 50 µM 2-propanol (as an $^\bullet OH$ scavenger) and varying concentrations of sodium sulfite. The illumination solutions were either prepared in MQ water or in a pH 8 phosphate buffer (0.010 M potassium phosphate monobasic in MQ water) where the pH was adjusted with sodium hydroxide or hydrochloric acid. Standards were prepared with sodium nitrite and contained the same concentration of S(IV) as the illumination solution. The Griess color development method was performed with either: (1) 25 µL of 1% (w/v) sulfanilamide in 10% (v/v) HCl/MQ solution and 25 µL of 0.1% (w/v) NED solution or (2) 50 µL of 1% (w/v) sulfanilamide in 30% (v/v) HCl/MQ and 50 µL of 0.1% (w/v) NED solution if the solution contained sulfite. Hydrogen peroxide was added to convert S(IV) to S(VI) in the reaction solutions and nitrite standards. Since H_2O_2 in the stock solution slowly decays, we monitored the concentration daily with a Shimadzu UV-2501PC spectrophotometer by monitoring the absorbance at 240 nm and using the base-10 molar absorption coefficient of 38.1 M^{-1} cm^{-1} (Miller and Kester, 1988). The Dionex check standard was made from the Dionex Combined Seven Anion Standard II diluted to 100-130 nM NO_2^-.

Illumination solutions were prepared from stock solutions of 0.10 M sodium nitrate, 0.10 M 2-propanol and 0.033 M sodium sulfite. The stock solutions of sodium nitrate and 2-propanol were prepared biannually and stored in amber bottles in a refrigerator. Both the sodium sulfite solutions and sodium nitrite standard curve standards were made fresh daily from their respective salt. The sulfanilamide and NED solutions were prepared monthly.

Section S2. Adapting the Griess Method for the Presence of Sulfite

A major problem with using S(IV) to convert NO_2 to NO_2^- is that S(IV) not only reacts with NO_2, but also other chemicals in solution. As shown in Figure S1, the addition of S(IV) to nitrite standards inhibits the Griess method of analysis by preventing the formation of the azo-dye, rendering spectroscopic analysis impossible. In contrast, sulfate, i.e., S(VI), does not interfere with the analysis of nitrite (Fig. S1). Therefore, oxidizing S(IV) to S(VI) after the conversion of NO_2 to NO_2^- but prior to the addition of the sulfanilamide reagent should allow us to accurately measure both nitrite and nitrogen dioxide production. We tried two different methods of oxidation: bubbling air into the solution and adding H_2O_2. Although bubbling air reduces the interference of S(IV) on nitrite determination, the relative standard error across replicate 100 nM NO_2^- standards is large (34%), and therefore this is not an appropriate method. In contrast, adding H_2O_2 to standard curve solutions containing S(IV) prior to the start of the Griess analysis effectively reduces the interference of S(IV) on nitrite measurements. The nitrite calibration curve regression line is linear and the 100 nM NO_2^- replicates are within 3% of each other. Therefore, we are able to measure nitrite in the presence of S(IV) by oxidizing the S(IV) to S(VI) with H_2O_2.

We then tested how the molar ratio of H_2O_2:S(IV) impacts both the linearity of the standard curve and the relative error among replicate standards. We tested molar ratios of 0.5:1, 1:1, 2:1, and 3:1 H_2O_2:S(IV). Both the 1:1 and 2:1 ratio standard curves have an R^2 greater than 0.99 while the corresponding values for the 0.5:1 and 3:1 ratio standard curves were less than 0.98. The 2:1 ratio provided triplicate 100 nM standard measurements that are within 5% of the true value and each other, while the 1:1: ratio 100 nM standard triplicates are within 15% of each other and the true value. Based on the excellent calibration curve linearity and replicate reproducibility, we use a 2:1 molar ratio of H_2O_2:S(IV).

We find that the nitrite signal in the presence of S(IV) and H_2O_2 is time sensitive, decaying by approximately 15% over the course of ~40 minutes after the addition of the NED solution. After this time, the error in the replicate standard and check standard are both greater than 10%, while after 4 hours there is no nitrite signal. We resolved this problem by immediately starting the UV-VIS analysis after waiting the necessary 10 minutes post NED addition, and by collecting all the UV-VIS spectra for a given set of samples within 20 minutes of recording the first sample spectrum. We also test both a 100 nM NO_2^- replicate standard and the Dionex check at the start and end of each batch of 8-10 samples to ensure that the signal does not change more than 10% throughout the analysis.

As shown in Figure S2, as the S(IV) concentration increases, the slope of the nitrite calibration curve regression line decreases. This could either be because of higher H_2O_2 (since we maintained a H_2O_2:S(IV) ratio of 2:1) or because of higher residual S(IV) after H_2O_2 addition. Although we are unsure whether S(IV), H_2O_2, or both are reacting with the sulfanilamide and/or NED reagents, we found that doubling the volume of the sulfanilamide and NED added to the samples produces a more linear calibration curve.

Another concern was that H_2O_2 could react with either nitrite, to form peroxynitrite, or the azo-dye, artificially decreasing the measured concentration of nitrite. However, we do not believe this is occurring under our conditions for the following reasons. In a pH 5 solution with 100 nM NO_2^- and 3 mM H_2O_2, the lifetime of NO_2^- is ~8.5 hours (~6 hour half-life) and the peroxynitrite formation rate would be 3.3 pM s^{-1} (Lukes et al., 2014). Since the azo-dye is formed from the Griess analysis within 20 minutes of the addition of H_2O_2, less than 5% of the nitrite would react with H_2O_2 during this time period. As discussed in section S3, we found the stability of the azo-dye to be 5 hours in the presence of H_2O_2. As long as the samples are analyzed within this 5-hour window, there should be no measurable destruction of the azo-dye by H_2O_2.

Because of the impact of S(IV) on the nitrite response, the calibration curve on a given day needs to contain the same S(IV) and H_2O_2 concentrations as the experimental solutions. With this procedure, the Dionex check standard and standard replicate give nitrite concentrations within 15% of their actual values, indicating that we can correct for the impacts of S(IV) and H_2O_2 on the nitrite response. However, the interference from S(IV) could be a problem at higher concentrations if the nitrite calibration curve becomes so flat that the regression line loses the required resolution for nitrite analysis.

Our final adaptation to the standard Griess method of analysis is in response to the effect of S(IV) on pH. The reaction of nitrite with Griess reagents to form the light-absorbing azo dye requires a pH below 2. Since the addition of 1.5 mM of Na_2SO_3 prevented the solution from becoming that acidic, we increased the acidity of the sulfanilamide solution from 10% to 30% hydrochloric acid, as recommend by Doane and Horwath (2003).

Section S3. Stability of Adapted Griess Reagent Samples

Here we consider the stability of the samples from sample treatments 1-3, which are described in Section 2.3 of the main text. The stability for sample treatment 1, i.e,. no S(IV) in solution, is known and the following considerations must be made. Once the nitrite has been generated in solution, the sample is stable for up to 28 days if kept refrigerated at 4 ˚C, otherwise it must be analyzed within 48 hours (Roman et al., 1991). Once the sulfanilamide has been added, the diazonium ion decays by ~2-3% per hour, therefore it is recommended to add the NED solution within 15 minutes of adding the sulfanilamide (Fox, 1979). There is no mention in the literature of the stability of the azo-dye once it has been formed, but based on our experiments it is stable for at least 4 hours on benchtop but is likely stable for longer.

Sample treatment 2, where S(IV) was present in solution during the illumination, is less stable than sample treatment 1. We found that after the nitrite was produced, the samples were stable for up to one week if kept refrigerated and covered at 4 ˚C. After the addition of H_2O_2, the samples were unstable after 5 minutes, so the sulfanilamide reagent needed to be added within this time for results to be precise and accurate. We did not test the stability of the diazonium ion formed after adding the sulfanilamide reagent, but after addition of the NED reagent, the samples were stable for up to 5 hours when left on the benchtop in the dark, and were found to degrade after 6 hours.

Sample treatment 3, where S(IV) was added to solution after illumination, had the same stability as sample treatment 2, except for one key difference, the addition of S(IV). Since this sample treatment adds S(IV) after illumination, the S(IV) must be added before the NO_2 decays or escapes from the illumination container. We found that we had to immediately inject the S(IV) into solution after stopping illumination. Waiting more than five minutes to add the S(IV) significantly decreased the NO_2 recovery.

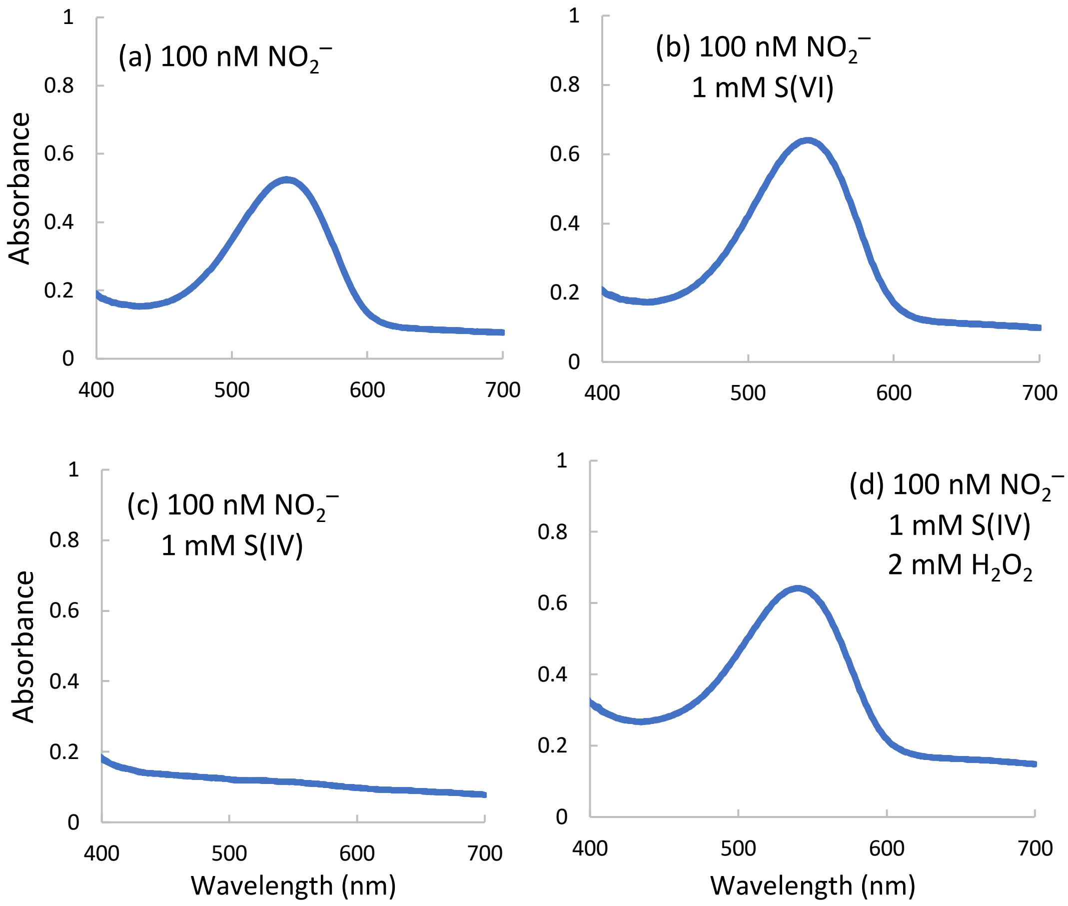

Figure S1. UV-VIS spectra for (a) 100 nM NO_2^-, (b) 100 nM NO_2^- and 1.0 mM sulfate (S(VI)), (c) 100 nM NO_2^- and 1.0 mM sulfite (S(IV)) and (d) 100 nM NO_2^-, 1.0 mM S(IV), and 2.0 mM H_2O_2. For panels (b) and (c), the sulfanilamide solution was added to start the Griess method of analysis within 5 and 10 minutes, respectively, after the preparation of the NO_2^- and S(VI) solution. For panel (d), the H_2O_2 was added within 3 min after the NO_2^- and sulfite solution was prepared, and the sulfanilamide reagent was added within 3 minutes after that.

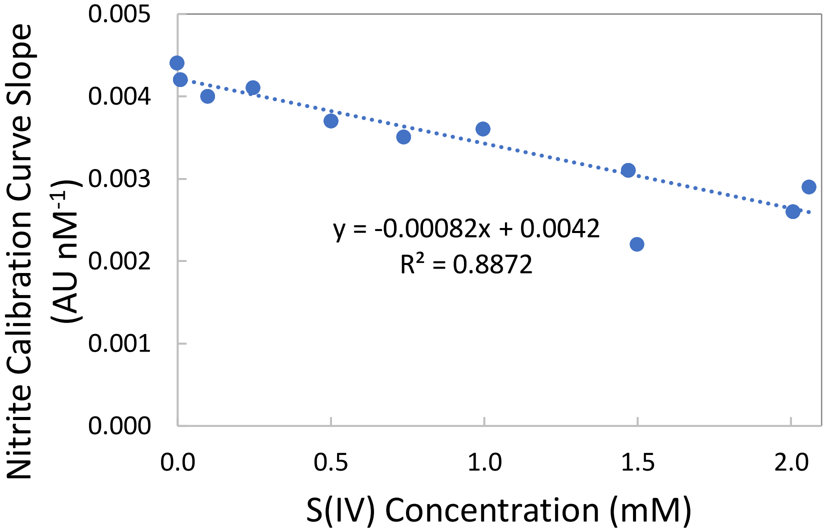

Figure S2. Impact of S(IV) concentration on the slope of the nitrite calibration curve. Each standard contained nitrite, the stated concentration of S(IV), and H_2O_2 at twice the S(IV) concentration.

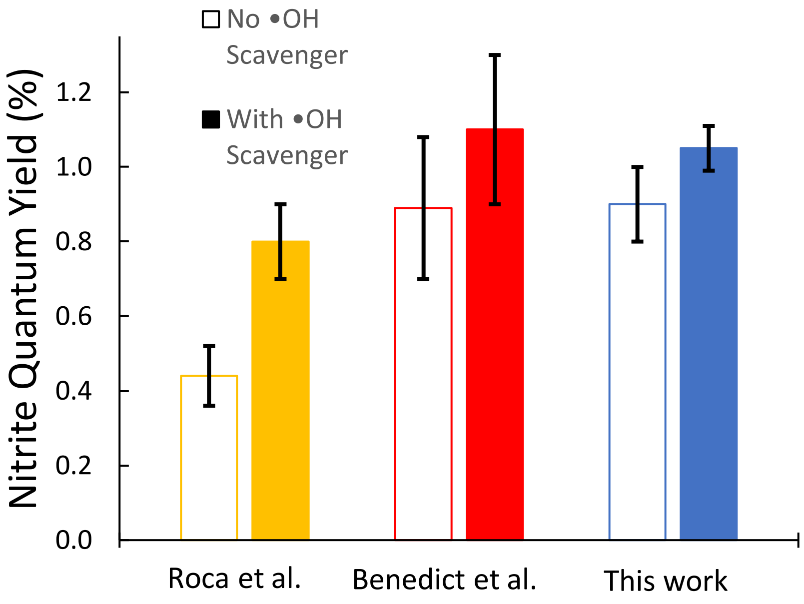

Figure S3. Influence of ${}^{\bullet}$OH scavenger on the nitrite quantum yield. Data are from: Roca et al. (2008) (yellow bars: 310 nm, 298 K, pH 4, 10 mM NO_3^-; no formate (hollow bar) or 10 mM formate (solid bar)); Benedict et al. (2017b) (red bars: 313 nm, 298 K, pH < 5, 50 µM NO_3^-; no formate or cysteine (hollow bar) and with 50 µM formate or cysteine (solid bar)); and this work (blue bars: 313 nm, 293 K, pH 5, 50 µM NO_3^-; no 2-propanol (hollow) or 50 µM 2-propanol (solid)). Error bars are ±1 σ for this work and Benedict et al., while the error bar for Roca et al. is their unspecified reported error.

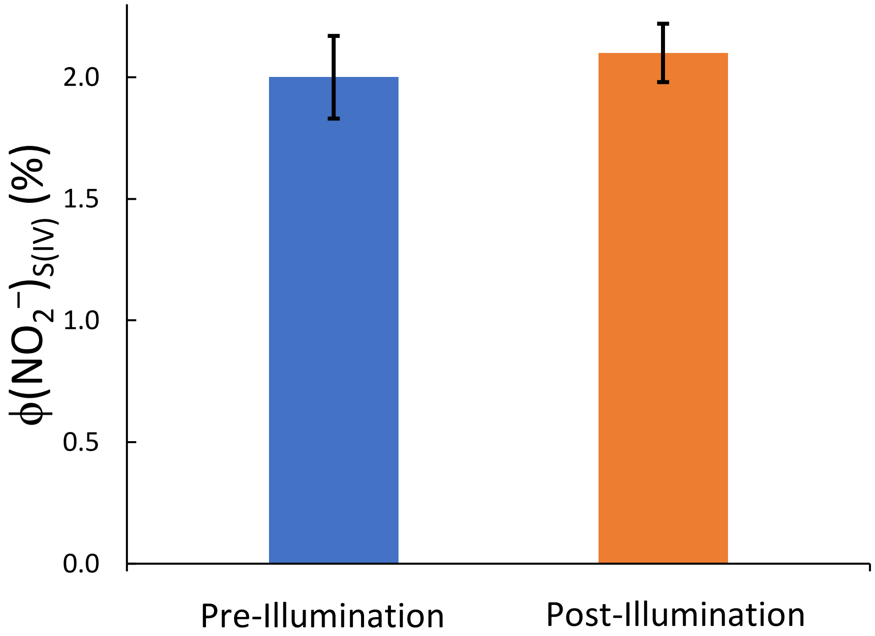

Figure S4. Comparison of the quantum yield for nitrite in the presence of S(IV) under two experimental conditions: (1) "Pre-Illumination", where 1.5 mM S(IV) was added to the solution prior to illumination or (2) "Post-Illumination", where 1.5 mM S(IV) was added after illumination. The quantum yields for the two conditions, (2.00 ± 0.14)% and (2.10 ± 0.08)%, respectively, are not statistically different (p = 0.16).

Table S1. Summary of literature values of $\Phi(NO_2)$ and $\Phi(NO_2^-)$ from aqueous nitrate photolysis

Study	Wavelength (nm)	Experiment Temp. (K)	Nitrate Concentration (μM)	Measured Quantum Yield	Quantum Yield at 293 K[a]
Determinations of hydroxyl radical quantum yields (channel 1)					
Zepp et al. (1987)	313	293	200-4000	1.30%	1.30%
Warneck & Wurzinger (1988)	305	295	10,000	0.92%	0.80%
Zellner et al. (1990)	308	298	3000	1.70%	1.50%
Chu and Anastasio (2003)	313	298	200	1.33%	1.20%
					Average (± 1 σ) $\phi(^{\bullet}OH) = 1.19 \pm 0.29\%$
Determinations of nitrite quantum yields from studies that used $^{\bullet}OH$ scavengers (channel 2)					
Warneck & Wurzinger (1988)	305	295	10,000	1.04%	1.01%
Goldstein & Rabani (2007)	300	297	20,000-100,000	0.94%	0.88%
Roca et al. (2008)	310	298	10,000	0.80%	0.74%
Benedict et al. (2017a)	313	293	50	1.14%	1.14%
Benedict et al. (2017b)	313	298	50	1.10%	1.02%
McFall et al. (2018)	313	298	50	0.93%	0.86%
					Average (± 1 σ) $\phi(NO_2^-) = 0.98 \pm 0.11\%$
					Average (± 1 σ) $(\phi(NO_2^-) + \phi(^{\bullet}OH)) = 2.17 \pm 0.52\%$

---

[a] Quantum yields not measured at 293 K were adjusted to this temperature with the Arrhenius equation using the activation energies from Chu et al. (2003), 20 kJ/mol, and Benedict et al. (2017b), 11 kJ/mol, for $\phi(^{\bullet}OH)$ and $\phi(NO_2^-)$, respectively.

Table S2. Conditions and $\phi(NO_2^-)_{S(IV)}$ measurements for experiments in Figures 1 and 2. All illuminations were performed with 50 µM $NaNO_3$, 313 nm illumination, and a temperature of 293 K.

Expt #	2-Propanol Concentration (µM)	S(IV) Concentration (µM)	Pre- or Post-Illumination S(IV) Addition	pH	j_{2NB} (s^{-1})	$\phi(NO_2^-)$ or $\phi(NO_2^-)_{S(IV)}$ (%)
1	0	0	N/A	4.9	0.0448	1.05
2	0	0	N/A	4.9	0.0448	0.94
3	0	0	N/A	4.9	0.0448	0.92
4	0	0	N/A	4.8	0.0469	0.79
5	0	0	N/A	4.8	0.0469	0.82
6	50	0	N/A	5.0	0.0485	1.13
7	50	0	N/A	4.9	0.0489	1.04
8	50	0	N/A	4.9	0.0489	1.07
9	50	0	N/A	4.9	0.0489	0.96
10	50	10	Pre	7.0	0.0415	1.21
11	50	10	Pre	7.0	0.0415	1.49
12	50	10	Pre	7.0	0.0415	1.38
13	50	100	Pre	7.8	0.0414	1.87
14	50	100	Pre	7.8	0.0414	1.53
15	50	100	Pre	7.8	0.0414	1.84
16	50	250	Pre	8.2	0.0423	1.87
17	50	250	Pre	8.2	0.0423	1.55
18	50	500	Pre	8.3	0.0403	2.08
19	50	500	Pre	8.3	0.0403	1.79
20	50	500	Pre	8.3	0.0403	2.00
21	50	750	Pre	8.3	0.0215	2.03
22	50	750	Pre	8.3	0.0215	1.93
23	50	750	Pre	8.3	0.0215	2.30
24	50	1000	Pre	8.2	0.0427	1.90

25	50	1000	Pre	8.2	0.0427	2.00
26	50	1000	Pre	8.2	0.0427	2.00
27	50	1500	Pre	8.6	0.0471	2.10
28	50	1500	Pre	8.6	0.0471	2.07
29	50	1500	Pre	8.6	0.0471	2.11
30	50	1500	Pre	8.6	0.0471	1.81
31	50	2000	Pre	8.6	0.0403	2.00
32	50	2000	Pre	8.6	0.0403	2.02
33	50	2000	Pre	8.6	0.0403	2.06
34	50	1500	Post	5.1	0.0489	2.09
35	50	1500	Post	5.1	0.0371	2.18
36	50	1500	Post	5.0	0.0494	2.03
36	0	1500	Post	5.1	0.0425	2.23
37	0	1500	Post	5.1	0.0399	2.13
38	0	1500	Post	5.0	0.0457	1.92

References

Benedict, K. B. and Anastasio, C.: Quantum Yields of Nitrite (NO_2^-) from the Photolysis of Nitrate (NO_3^-) in Ice at 313 nm, J. Phys. Chem. A, 121, 8474–8483, https://doi.org/10.1021/acs.jpca.7b08839, 2017.

Benedict, K. B., McFall, A. S., and Anastasio, C.: Quantum Yield of Nitrite from the Photolysis of Aqueous Nitrate above 300 nm, Environ. Sci. Technol., 51, 4387–4395, https://doi.org/10.1021/acs.est.6b06370, 2017.

Chu, L. and Anastasio, C.: Quantum Yields of Hydroxyl Radical and Nitrogen Dioxide from the Photolysis of Nitrate on Ice, J. Phys. Chem. A, 107, 9594–9602, https://doi.org/10.1021/jp0349132, 2003.

Doane, T. A. and Horwath, W. R.: Spectrophotometric Determination of Nitrate with a Single Reagent, Analytical Letters, 36, 2713–2722, https://doi.org/10.1081/AL-120024647, 2003.

Fox, J. B.: Kinetics and mechanisms of the Griess reaction, Anal. Chem., 51, 1493–1502, https://doi.org/10.1021/ac50045a032, 1979.

Goldstein, S. and Rabani, J.: Mechanism of Nitrite Formation by Nitrate Photolysis in Aqueous Solutions: The Role of Peroxynitrite, Nitrogen Dioxide, and Hydroxyl Radical, J. Am. Chem. Soc., 129, 10597–10601, https://doi.org/10.1021/ja073609+, 2007.

Lukes, P., Dolezalova, E., Sisrova, I., and Clupek, M.: Aqueous-phase chemistry and bactericidal effects from an air discharge plasma in contact with water: evidence for the formation of peroxynitrite through a pseudo-second-order post-discharge reaction of H_2O_2 and HNO_2, Plasma Sources Sci. Technol., 23, 015019, https://doi.org/10.1088/0963-0252/23/1/015019, 2014.

McFall, A. S., Edwards, K. C., and Anastasio, C.: Nitrate Photochemistry at the Air–Ice Interface and in Other Ice Reservoirs, Environ. Sci. Technol., 52, 5710–5717, https://doi.org/10.1021/acs.est.8b00095, 2018.

Miller, W. L. and Kester, D. R.: Hydrogen peroxide measurement in seawater by (p-hydroxyphenyl)acetic acid dimerization, Anal. Chem., 60, 2711–2715, https://doi.org/10.1021/ac00175a014, 1988.

Roca, M., Zahardis, J., Bone, J., El-Maazawi, M., and Grassian, V. H.: 310 nm Irradiation of Atmospherically Relevant Concentrated Aqueous Nitrate Solutions: Nitrite Production and Quantum Yields, J. Phys. Chem. A, 112, 13275–13281, https://doi.org/10.1021/jp809017b, 2008.

Roman, M., Dovi, R., Yoder, R., Dias, F., and Warden, B.: Determination by ion chromatography and spectrophotometry of the effects of preservation on nitrite and nitrate, Journal of Chromatography A, 546, 341–346, https://doi.org/10.1016/S0021-9673(01)93032-8, 1991.

Warneck, P. and Wurzinger, C.: Product quantum yields for the 305-nm photodecomposition of nitrate in aqueous solution, J. Phys. Chem., 92, 6278–6283, https://doi.org/10.1021/j100333a022, 1988.

Zellner, R., Exner, M., and Herrmann, H.: Absolute OH quantum yields in the laser photolysis of nitrate, nitrite and dissolved H_2O_2 at 308 and 351 nm in the temperature range 278–353 K, J Atmos Chem, 10, 411–425, https://doi.org/10.1007/BF00115783, 1990.

Zepp, R. G., Hoigné, J., and Bader, H.: Nitrate-induced photooxidation of trace organic chemicals in water, Environ. Sci. Technol., 21, 443–450, https://doi.org/10.1021/es00159a004, 1987.